Downloaded 07/04/17 to 134.153.188.68. Redistribution subject to SEG license or copyright; see Terms of Use at http://library.seg.org/

The role of cracks in the nonlinear interaction of a P-wave with an S-wave

Alison Malcolm, Memorial University, St John's, Canada, James TenCate, Los Alamos National Laboratory, Michael Fehler, Earth Resources Laboratory, MIT

SUMMARY

Cracks play a key role in our ability to produce oil and gas, from micro-scale cracks that enable permeability in tight formations to faults and fractures that compartmentalize reservoirs; our ability to sense and understand them remotely is thus of key importance. We explore the role that cracks play in the nonlinear interaction of propagating waves. We present a laboratory experiment in which a strong S-wave slightly changes the velocity of a lower amplitude P-wave, and use a rock sample with aligned fractures to demonstrate that this signal is strongly dependent on fracture orientation. We build on the linear slip theory to show that the propagating S-wave is indeed able to open the cracks that the P-wave velocity will be most sensitive to. This gives firm, direct evidence that cracks are a controlling factor in the nonlinear elastic properties of rocks, and opens up the possibility of using such signals to remotely map fracture orientations.

INTRODUCTION

Understanding cracks is of key importance in a variety of different exploration situations. In large-scale conventional oil and gas plays, faults and fractures compartmentalize reservoirs; in unconventional and geothermal energy, fractures can be the primary porosity and permeability. Directly characterizing fractures is difficult, however, as they tend to generate complicated signatures on seismic data such as anisotropy (Thomsen, 1995), multiple-scattering (Willis et al., 2006) or specific wavenumber properties (Fang et al., 2013). In this work, we present a laboratory scale experiment that highlights how fracture orientation influences the nonlinear interaction of a P-wave with an S-Wave.

The experiment builds on work in Gallot et al. (2014, 2015) in which we use a low-amplitude P-wave as a probe to measure the effect of a strong S-wave pump on a rock sample. The design of our experiment has similarities with past work on the interaction of two P-waves in both solids and fluids (Zverev and Kalachev, 1970; Ichida et al., 1983; TenCate et al., 1996). It is also closely related to the Dynamic Acousto-Elastic Testing (DAET) method (Renaud et al., 2009, 2011, 2012a), with the difference being that DAET works in the resonance regime, whereas we look at propagating waves.

Nonlinear elasticity has been used to characterize rocks for a number of years (Johnson et al., 1991; D Angelo et al., 2004; Renaud et al., 2012b), and some work has been done to understand how fractures influence this nonlinear signal. The recent modeling work of Pecorari (2015) looks at what nonlinear effects can be explained by different fracture boundary properties. Van Den Abeele et al. (2009) look at the correlation of the nonlinear signal with fracture density. There is ample literature on using the nonlinear elasticity to locate and characterize fractures for non-destructive testing (see e.g. Jhang (2009) for a recent overview). What is missing is the definitive experiment in a rock sample that highlights the impact of fractures independent of other parameters. In this paper, we present such an experiment.

To highlight the impact of fractures, and their orientation, on the nonlinear interaction of the two waves, we use a sample called Crab Orchard Sandstone that is shown by Benson et al. (2005) to have a set of aligned fractures. We perform the experiment on two different samples. In each sample, we compare the nonlinear signal recorded in two directions by rotating the sample relative to the measurement apparatus. The first sample, Sample 1, is cut so that the fracture orientations change relative to the particle motion direction of the pump and probe when the sample is rotated. Sample 2 is cut so that the fracture orientations do not change, relative to the particle motion of the waves, when it is rotated (see Figure 1). In this way, Sample 2 acts as a control, showing that the observed difference in the nonlinear signal is not from the experimental design but instead is likely from the change in the orientations of the fractures relative to the particle motion of the pump and probe.

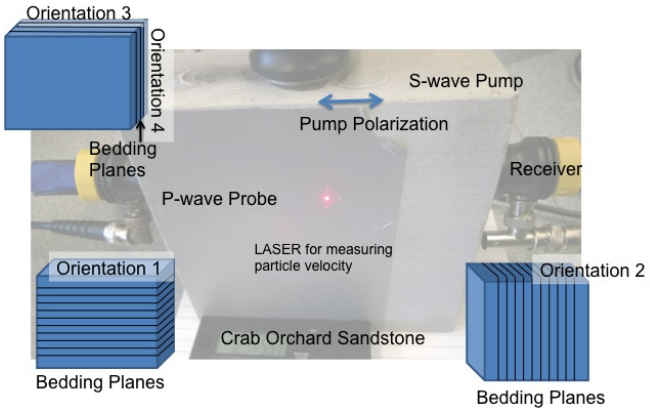

Figure 1: Experimental setup.

In our experiment, a vertically propagating large amplitude S-wave (the 'pump') slows down a horizontally propagating low amplitude P-wave (the 'probe'). Our observations show that the strenght of this effect depends on the relative orientation of fractures and the particle motion of the waves (the particle motions of the two waves are aligned). We expect that the slow-down in the probe traveltime is caused by the opening of fractures in which the normal to the crack face is aligned with the particle motion, and the resulting softening of the rock structure. It is not obvious however that our S wave pump can indeed open such cracks, whose normal would also be aligned with the particle motion of this wave. To test this, we give simple linear slip calculations (Schoenberg, 1980) showing that under the conditions expected in our experiment we would indeed expect the S-wave to open these cracks.

EXPERIMENTAL DESIGN

The experimental setup, shown in Figure 1, is essentially the same as that described by Gallot et al. (2014, 2015); we give a brief description here of the most important aspects.

As mentioned above, our aim is to measure the interaction of two waves, and to improve our understanding of fractures and their orientations on that interaction. To that end, we use an experiment in which we have two waves, propagating perpindicular to one another, but with their particle motions aligned. One of these waves, the low-frequency (50-75 kHz) S-wave pump shown propagating vertically in Figure 1 is of sufficiently high amplitude (strains on the order of 10^{-6}), that it perturbs the elastic properties of the rock. We call this wave the pump. The second wave, the P-wave shown propagating horizontally in Figure 1, is smaller (strains on the order of 10^{-8}) and higher fre-

© 2016 SEG

Downloaded 07/04/17 to 134.153.188.68. Redistribution subject to SEG license or copyright; see Terms of Use at http://library.seg.org/

quency (700-1000 kHz) and is used to sense these changes. Specifically, we measure the delay in the P-wave probe caused by the S-wave pump. The precise frequency of the probe and pump signals are tuned to acheive a high signal-to-noise ratio and a pulse with as little ringing as possible. We aim to keep approximately a factor of 10 difference in frequency between the two waves so that we can reasonably assume that the probe is seeing a single phase of the pump during the wave interaction.

The delays induced in the P-wave probe by the S-wave pump are small, with the induced velocity change being on the order of 0.04%. To measure such small delays requires a careful experimental setup. This setup is described in detail by Gallot et al. (2015) and refined in this work both using the same equipment as that in Gallot et al. (2015) at MIT and using similar equipment at Memorial University. Both the pump and probe signals are generated by transducers connected to a function generator, which also controls the timing between these two signals. The pump signal is amplified to generate a large enough signal using a fixed gain power amplifier; no amplification is used on the probe signal. All of the signals are recorded on a P-wave transducer directly opposite the probe source transducer; before recording a bandpass filter is used to reduce the amplitude of the pump, allowing clear signals of the probe to be recorded above the bit noise of the oscilloscope that does the recording.

Each data point is a delay in the probe traveltime caused by the pump signal. To measure this delay time, we make three separate measurements. First, we record the probe signal with the pump transducer inactive, this generates our baseline signal, S_1. Second, we record only the S-wave pump signal (still on the P-wave transducer opposite to the P-wave probe source); we call this signal S_2. Third, we record both signals together (i.e. with both the pump and probe transmitting at the same time), which is our nonlinear mixing signal S_3. We then form the perturbed probe signal via

$$S_1' = S_3 - S_2 \,.$$

We can now measure the delay by comparing the traveltime of S_1 to that of S_1'. As mentioned above, the traveltime delays we aim to measure are small, on the order of our time sampling interval (all data were sampled with at most 4 ns sampling interval). To measure such small delays, we make use of a technique discussed by e.g. Catheline et al. (1999), in which we first cross-correlate the two probe signals

$$S_{CC} = S_1' * S_1$$

where $*$ is the cross-correlation, and then fit the peak of the cross-correlation to a parabola. The measured delay is then the peak of this interpolated parabola. This allows us to make delay measurements at about 1/10 of the sampling interval. This process gives us a single data point on the plots shown in subsequent sections.

To generate a full data set, we then repeat the procedure described above as a function of the delay between the probe initiation time and the pump initiation time. By changing this delay, we change the phase of the high-amplitude pump signal that is seen by the probe. This allows us to sense the passing of the pump using the delay of the probe as a measuring tool. To ensure that the probe really does see primarily a single phase of the pump, we use a single cycle of the high-frequency probe and monitor the passage of several cycles of the low-frequency pump.

As mentioned in the introduction, we perform this experiment in two samples of Crab Orchard Sandstone; the samples are shown in Figure 1 and each is 15×15 cm in size. In Sample 1, we can change the orientation of the fractures relative to the particle motion of the waves (recall that the S-wave particle motion is chosen to align with that of the P-wave), by turning the sample 90° while keeping the pump and probe locations fixed. In Sample 2, changing the orientation of the sample does not change the relative orientation of the fractures and the particle motion, thus providing a control measurement. Thus any changes observed in Sample 1 that are not seen in Sample 2 can be hypothesized to be caused by the differences in the relative orientation of the wave particle motions and the bedding planes (and thus the fractures). The sample orientations relative to the bedding planes and thus fracture planes, are shown in Figure 1. We expect the changes in probe traveltime to be caused by the opening and closing of those fractures which have the normal to the crack face aligned with the P-wave probe particle motion. The following section argues that the S-wave pump will indeed open such fractures.

LINEAR SLIP THEORY FOR THE S-WAVE PUMP

We use the linear slip theory of Schoenberg (1980) to argue that the S-wave pump can open fractures that have the normal to the crack face aligned with their particle motion. In particular, we address whether an S-wave propagating along the vertical, z-axis as shown in Figure 1, with particle motion along the horizontal x–axis can open horizontal cracks (crack-face along the x–axis) and vertical cracks (crack-face along the $z-axis$). The two different crack orientations represent the two orientations of Sample 1. We discuss three cases: (i) a plane wave in a linear elastic material (ii) a plane wave windowed in the x–direction in a linearly elastic material and (iii) a plane wave in a material described by the 5-constant nonlinear elastic model (Gol'dberg, 1960) and calculate the displacement across the crack face for both fracture orientations in each case. We describe the derivation for case (i) and then discuss the changes between those results and those in case (ii) and (iii).

The displacement u caused by a vertically propagating plane S-wave with amplitude K is

$$u = \begin{pmatrix} Ke^{i\omega(\frac{z}{\beta}-t)} \\ 0 \\ 0 \end{pmatrix}, \tag{1}$$

where β is the S-wave speed, t the time and ω the angular frequency. This formulation assumes a plane-wave of infinite extent in x and y. For the two cases of fracture orientations we are interested in, we have

$$n_v = \begin{pmatrix} 1 \\ 0 \\ 0 \end{pmatrix}, \; n_h = \begin{pmatrix} 0 \\ 0 \\ 1 \end{pmatrix}, \tag{2}$$

where n_v is the normal to the vertical fracture (i.e. orientation 2) and n_h is the normal to the horizontal fracture (i.e. orientation 1). Linear slip says that

$$\Delta u_v = \begin{pmatrix} \eta_N & 0 & 0 \\ 0 & \eta_T & 0 \\ 0 & 0 & \eta_T \end{pmatrix} t_v \tag{3}$$

$$\Delta u_h = \begin{pmatrix} \eta_T & 0 & 0 \\ 0 & \eta_T & 0 \\ 0 & 0 & \eta_N \end{pmatrix} t_h \tag{4}$$

where Δu is the displacement (or slip) across the fracture, η_T and η_N are the tangential and normal tractions, respectively and $t_{v,h}$ are the tractions on the fractures. Using linear elasticity and the Cauchy stress formula to obtain expressions for t gives that

$$\Delta u_v = \begin{pmatrix} 0 \\ 0 \\ \eta_T \mu K \frac{i\omega}{\beta} e^{i\omega(\frac{z}{\beta}-t)} \end{pmatrix} \tag{5}$$

$$\Delta u_h = \begin{pmatrix} \eta_T \mu K \frac{i\omega}{\beta} e^{i\omega(\frac{z}{\beta}-t)} \\ 0 \\ 0 \end{pmatrix}, \tag{6}$$

© 2016 SEG

Downloaded 07/04/17 to 134.153.188.68. Redistribution subject to SEG license or copyright; see Terms of Use at http://library.seg.org/

where λ and μ are the Lamé constants.

The calculation above indicates that in this situation, the shear wave in our experiment will not open the cracks, because there is no displacement along the normal to the crack face (i.e. $\Delta u \cdot n = 0$). This changes, however, if we assume:

- A windowed plane wave in which

$$\mathbf{u} = \begin{pmatrix} s(x)Ke^{i\omega(\frac{z}{\beta}-t)} \\ 0 \\ 0 \end{pmatrix}, \tag{7}$$

  where $s(x)$ is a windowing function that is one at the transducer that smoothly decays to zero away from it. This gives

$$\Delta u_v = \begin{pmatrix} \eta_N(\lambda+2\mu)s'(x) \\ 0 \\ \eta_T \mu \frac{i\omega}{\beta} s(x) \end{pmatrix} Ke^{i\omega(\frac{z}{\beta}-t)} \tag{8}$$

$$\Delta u_h = \begin{pmatrix} \eta_T \mu s(x) \frac{i\omega}{\beta} \\ 0 \\ \eta_N \lambda s'(x) \end{pmatrix} Ke^{i\omega(\frac{z}{\beta}-t)}, \tag{9}$$

  in which we see that both displacements have a component along the normal direction.

- A compliance tensor that is not diagonal as it is in equation 4
- A nonlinear Hooke's law in computing the tractions t_h and t_v from the stresses in equation 4

The last two cases give similar, but more complicated, expressions for Δu_v and Δu_h, where the form of each component changes but which are nonzero does not. We can thus conclude that if any of the above deviations from the ideal linear elastic case hold, the S-wave pump would be expected to produce an opening of the cracks in sample orientations 1 and 2. For orientations 3 and 4 (in which the crack orientations are expected to be the same relative to the particle motions of both pump and probe), using a more complicated compliance model does not result in the opening and closing of fractures, but the other modifications mentioned above do result in crack opening and closing. Which cracks open more or less is governed by the precise values of tractions and physical parameters of the rock, and is unimportant for our study. This simple calculation gives us confidence that the pump can open the fractures with normals parallel to the particle motions; it is these fractures that are most likely to perturb the traveltime of the P-wave.

EXPERIMENTAL RESULTS

Having established that our experimental setup allows for the opening and closing of cracks, we now procede to describe the results of the experiments described above. Figure 2 shows the results in Sample 1, in orientations 1 and 2. Recall that in orientation 1, the particle motion is parallel to the bedding planes and thus the fracture planes. In orientation 2, the opposite is true and the particle motion is perpendicular to the bedding planes and the fracture planes (i.e. the particle motion is aligned with the normals to the fractures). The P-wave motion is going to be most strongly effected by opening and closing of fractures whose normals are aligned with the direction of wave propagation, in other words fractures aligned as in orientation 2. We thus expect, and observe, a stronger nonlinear effect in orientation 2 than in orientation 1. Note that in both cases, the two waves interfere in nearly the same part of the sample, so it is unlikely that these results demonstrate only the heterogeneity of the sample.

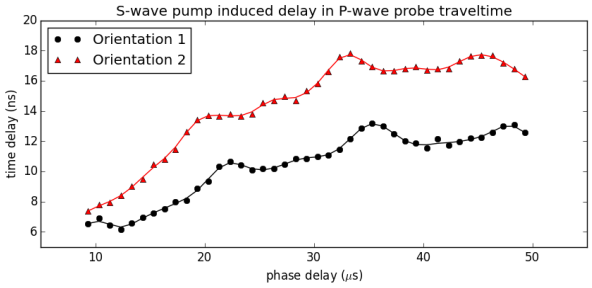

Figure 2: Experimental results on Sample 1, in orientations 1 and 2. Note the difference in the time delays measured in the two orientations. In this sample, the relative orientation of the cracks does change when the sample is rotated, resulting in the change in observed time delays. In orientation 2, the particle motion of the waves and the normal to the crack faces are aligned, which is why we observe a larger signal in that orientation.

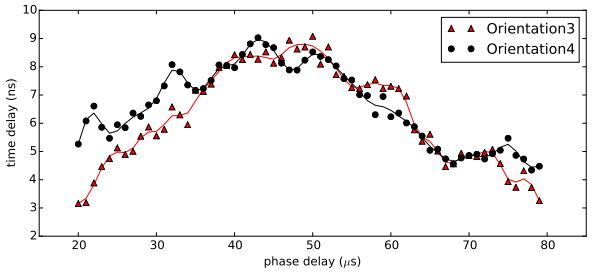

Figure 3: Experimental results on Sample 2, in orientations 3 and 4. Note the similarity in the time delays measured in the two orientations. In this sample, the relative orientation of the cracks and wave particle motions does not change when the sample is rotated.

In contrast, in Figure 3 we show the experimental results in Sample 2 with orientations 3 and 4. In this case, we observe little difference in the time delays for the two orientations. This is expected because in this case, there is no change in the relative orientation of the fractures and particle motion when the sample is rotated. Note that since we are using two different samples, and making measurements in two dif-

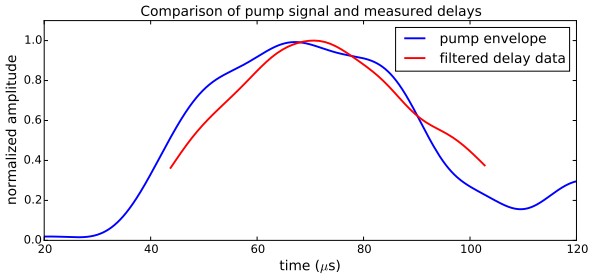

Figure 4: The envelope of the pump signal, recorded on an S-wave transducer opposite the pump transducer, and the low-pass filtered delays measured on Sample 2 in Orientation 3. Note the similarity in shape of the two signals, with the envelope of the nonlinear signal slightly lagging that of the pump. This is the part of the signal that changes between orientations in Sample 1, likely due to differences in how the pump and probe interact with the aligned fractures in the sample.

© 2016 SEG

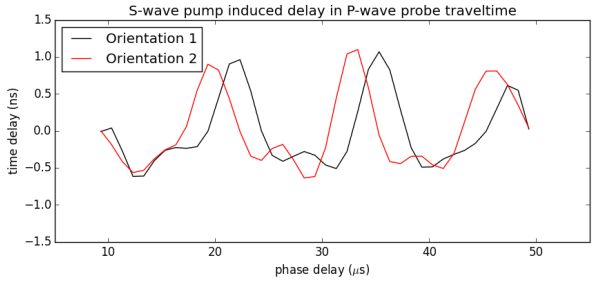

Figure 5: High-pass filtered version of the data shown in Figure 2 collected on Sample 1 in orientations 1 and 2. Note that despite the differences in the time delays shown in Figure 2, this component remains quite similar. The reason why this is the case is the subject of further investigations.

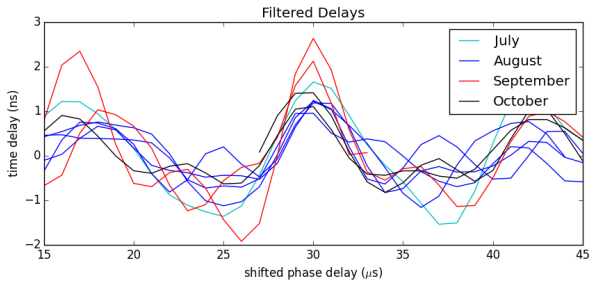

Figure 6: Data collected in Sample 1 on different dates, filtered to show only the component of the signal at the pump frequency. Note the difference in the amplitude of this component of the signal in different months. We are investigating the correlation of higher amplitudes of this component of the signal with higher humidity.

ferent labs several months apart we would not expect to see the same absolute delay times between the two samples, although we would expect to see similar trends. Care was taken in all measurements to appropriately match the amplitudes of the pump and probe signals between each pair of experiments.

It is clear that the nonlinear signal has two components, one at approximately the pump frequency and another at a lower frequency. The signal at the lower frequency is well-approximated by the envelope of the pump signal as illustrated in Figure 4 for data collected on Sample 2. This is likely a slow-dynamics (Ten Cate and Shankland, 1996) effect, related to the amount of time it takes for cracks to be perturbed by the passage of the pump. It is this signal that changes between the two orientations of the sample.

The second signal, at the pump frequency does not appear to change significantly with the sample orientation, as illustrated in Figure 5, in which the lower-frequency signal has been filtered out. These wiggles do appear to be sensitive to room conditions, however, as evidenced by the data in Figure 6. This figure shows a filtered version of data collected at different times in the MIT lab and have been aligned so that the largest peak of each data set is in the center of the figure and colored by the month in which they were collected. (Within each month all data were collected over a period of 4-5 days.) We have noted that the amplitude of this signal seems to be stronger in September and July, when the local humidity was notably higher than in August and October. Further work on this topic is ongoing to determine whether these preliminary observations are robust.

CONCLUSIONS

We have shown that the nonlinear coupling of two waves is dependent on the relative orientation of the cracks in the sample and the particle motion of the sensing waves. Our evidence is in the difference in the observed nonlinear signal when this relative orientation is varied. We have also shown that under conditions expected to hold in our experiment the vertically propagating S-wave pump will be able to open cracks with the normal to the crack face aligned with the P-wave.

ACKNOWLEDGMENTS

This study was supported by Weatherford to MF and AM and by Chevron and with grants from the Natural Sciences and Engineering Research Council of Canada Industrial Research Chair Program and the Research and Development Corporation of Newfoundland and Labrador and by the Hibernia Management and Development Corporation awarded to AM and colleagues. We are grateful to Steve Brown, Dan Burns and Xuan Feng of MIT and to John Hallman and Ingo Geldmacher of Weatherford for useful discussions.

Downloaded 07/04/17 to 134.153.188.68. Redistribution subject to SEG license or copyright; see Terms of Use at http://library.seg.org/

© 2016 SEG

Downloaded 07/04/17 to 134.153.188.68. Redistribution subject to SEG license or copyright; see Terms of Use at http://library.seg.org/

EDITED REFERENCES

Note: This reference list is a copyedited version of the reference list submitted by the author. Reference lists for the 2016 SEG Technical Program Expanded Abstracts have been copyedited so that references provided with the online metadata for each paper will achieve a high degree of linking to cited sources that appear on the Web.

REFERENCES

Benson, P., P. Meredith, E. Platzman, and R. White, 2005, Pore fab-ric shape anisotropy in porous sandstones and its relation to elastic wave velocity and permeability anisotropy under hydrostatic pressure: International Journal of Rock Mechanics and Mining Sciences, **42**, 890–899, http://dx.doi.org/10.1016/j.ijrmms.2005.05.003.

Catheline, S., F. Wu, and M. Fink, 1999, A solution to diffraction bi- ases in sonoelasticity: The acoustic impulse technique: The Journal of the Acoustical Society of America, **105**, no. 5, 2941–2950, http://dx.doi.org/10.1121/1.426907.

Angelo, D., R. K. Winkler, T. Plona, B. Landsberger, and D. Johnson, 2004, Test of hyperelasticity in highly nonlinear solids: Sedimen- tary rocks: Physical Review Letters, **93**, 214301, http://dx.doi.org/10.1103/PhysRevLett.93.214301.

Fang, X., M. C. Fehler, Z. Zhu, Y. Zheng, and D. R. Burns, 2013, Reservoir fracture characterization from seismic scattered waves: Geophysical Journal International, **196**, 481–492, http://dx.doi.org/10.1093/gji/ggt381.

Gallot, T., A. Malcolm, D. Burns, S. Brown, M. Fehler, and T. Szabo, 2014, Nonlinear interaction of seismic waves in the lab: A potential tool for characterizing pore structure and fluids: 84th Annual International Meeting, SEG, Expanded Abstracts, 2743–2748, http://dx.doi.org/10.1190/segam2014-0248.1.

Gallot, T., A. Malcolm, T. Szabo, S. Brown, D. Burns, and M. Fehler, 2015, Characterizing the nonlinear interaction of S- and P-waves in a rock sample: Journal of Applied Physics, **117**, 034902, http://dx.doi.org/10.1063/1.4905913.

Gol'dberg, Z., 1960, Interaction of plane longitudinal and transverse elastic waves: Soviet Physics Acoustics, **6**, 307–310.

Ichida, N., T. Sato, and M. Linzer, 1983, Imaging the nonlinear ultra- sonic parameter of a medium: Ultrasonic Imaging, **5**, 295–299.

Jhang, K. Y., 2009, Nonlinear ultrasonic techniques for non- destructive assessment of micro damage in material: A review: International Journal of Precision Engineering and Manufacturing, **10**, 123–135, http://dx.doi.org/10.1007/s12541-009-0019-y

Johnson, P. A., A. Migliori, and T. J. Shankland, 1991, Continuous wave phase detection for probing nonlinear elastic wave interactions in rocks: The Journal of the Acoustical Society of America, **89**, 598–603, http://dx.doi.org/10.1121/1.400384.

Pecorari, C., 2015, Modeling the elasto-acoustic hysteretic nonlinearity of dry Berea sandstone: Wave Motion, **52**, 66–80, http://dx.doi.org/10.1016/j.wavemoti.2014.09.001.

Renaud, G., S. Calle, and M. Defontaine, 2009, Remote dynamic acoustoelastic testing: Elastic and dissipative acoustic nonlineari- ties measured under hydrostatic tension and compression: Applied Physics Letters, **94**, 011905, http://dx.doi.org/10.1063/1.3064137.

Renaud, G., P.-Y. Le Bas, and P. A. Johnson, 2012a, Revealing highly complex elastic nonlinear (anelastic) behavior of Earth materials applying a new probe: Dynamic acoustoelastic testing: Journal of Geophysical Research, **117**, B06202, http://dx.doi.org/10.1029/2011JB009127.

Renaud, G., P.-Y. Le Bas, and P. A. Johnson, 2012b, Revealing highly complex elastic nonlinear (anelastic) behavior of Earth materials applying a new probe: Dynamic acoustoelastic testing: Journal of Geophysical Research: Solid Earth (1978–2012), 117, http://dx.doi.org/10.1029/2011JB009127.

© 2016 SEG

Renaud, G., M. Talmant, S. Callé, M. Defontaine, and P. Laugier, 2011, Nonlinear elastodynamics in micro-inhomogeneous solids observed by head-wave based dynamic acoustoelastic testing: The Journal of the Acoustical Society of America, **130**, 3583–3589, http://dx.doi.org/10.1121/1.3652871.

Schoenberg, M., 1980, Elastic wave behavior across linear slip inter- faces: The Journal of the Acoustical Society of America, **68**, 1516–1521, http://dx.doi.org/10.1121/1.385077.

Ten Cate, J., and T. Shankland, 1996, Slow dynamics in the nonlinear elastic response of Berea sandstone: Geophysical Research Letters, **23**, 3019–3022, http://dx.doi.org/10.1029/96GL02884.

TenCate, J. A., K. E. A. Van Den Abeele, T. J. Shankland, and P. A. Johnson, 1996, Laboratory study of linear and nonlinear elastic pulse propagation in sandstone: The Journal of the Acoustical Society of America, **100**, 1383, http://dx.doi.org/10.1121/1.415985.

Thomsen, L., 1995, Elastic anisotropy due to aligned cracks in porous rock: Geophysical Prospecting, **43**, 805–829, http://dx.doi.org/10.1111/j.1365-2478.1995.tb00282.x.

Van Den Abeele, K., P. Y. Le Bas, B. Van Damme, and T. Katkowski, 2009, Quantification of material nonlinearity in relation to micro- damage density using nonlinear reverberation spectroscopy: Experimental and theoretical study: The Journal of the Acoustical Society of America, **126**, 963–972, http://dx.doi.org/10.1121/1.3184583.

Willis, M. E., D. R. Burns, R. Rao, B. Minsley, M. N. Toksoz, and L. Vetri, 2006, Spatial orientation and distribution of reservoir fractures from scattered seismic energy: Geophysics, **71**, no. 5, O43–O51, http://dx.doi.org/10.1190/1.2235977.

Zverev, A., and A. Kalachev, 1970, Modulation of sound by sound in the intersection of sound waves: Soviet Physics Acoustics, 16.

Downloaded 07/04/17 to 134.153.188.68. Redistribution subject to SEG license or copyright; see Terms of Use at http://library.seg.org/